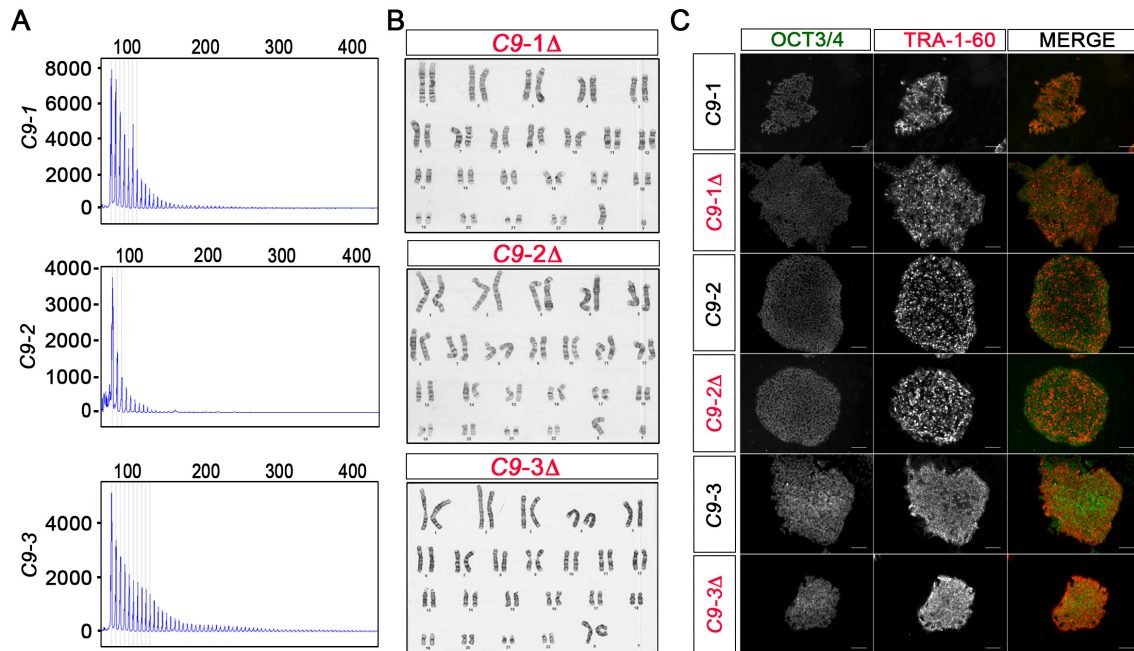


Supplementary Figure 1

**D**

C9-gRNA-1 sequence : AACTCAGGAGTCGCGCGCTA

C9_Fw_chr2:-231921408 : AGGTCAGGAGTCCGCGCAA

Control AAACCTCCTCGAGGTCAGGAGTCCCGCGCAACGGAACACTGGTCT

C9-1Δ AAACCTCCTCGAGGTCAGGAGTCCCGCGCAACGGAACACTGGTCT

C9-2Δ AAACCTCCTCGAGGTCAGGAGTCCCGCGCAACGGAACACTGGTCT

C9-3Δ AAACCTCCTCGAGGTCAGGAGTCCCGCGCAACGGAACACTGGTCT

C9_Fw_chr7:-151551819 : ATCACAGGAGGCGCGCCCTA

Control GTTGTGTGAGAATCACAGGAGGCGCGCCCTAAGGACCAGGCACCC

C9-1Δ GTTGTGTGAGAATCACAGGAGGCGCGCCCTAAGGACCAGGCACCC

C9-2Δ GTTGTGTGAGAATCACAGGAGGCGCGCCCTAAGGACCAGGCACCC

C9-3Δ GTTGTGTGAGAATCACAGGAGGCGCGCCCTAAGGACCAGGCACCC

C9-gRNA-2 sequence : GGCCCGCCCGACCAGGCC

C9_Rev_chr3:+98241587_NM_001040199 : CGCCAGCCCGACCAGGCC

Control CGCTCGGAACCCGCCAGCCCGACCAGCCCGGGAAGGGGGCCCC

C9-1Δ CGCTCGGAACCCGCCAGCCCGACCAGCCCGGGAAGGGGGCCCC

C9-2Δ CGCTCGGAACCCGCCAGCCCGACCAGCCCGGGAAGGGGGCCCC

C9-3Δ CGCTCGGAACCCGCCAGCCCGACCAGCCCGGGAAGGGGGCCCC

C9_Rev_chr22:-37731099 : GCCCGCTCCGCCACGCC

Control TTCTTCCTGGATGCCCGCTCCGCCACGCCCAAGTTCTCCGGCA

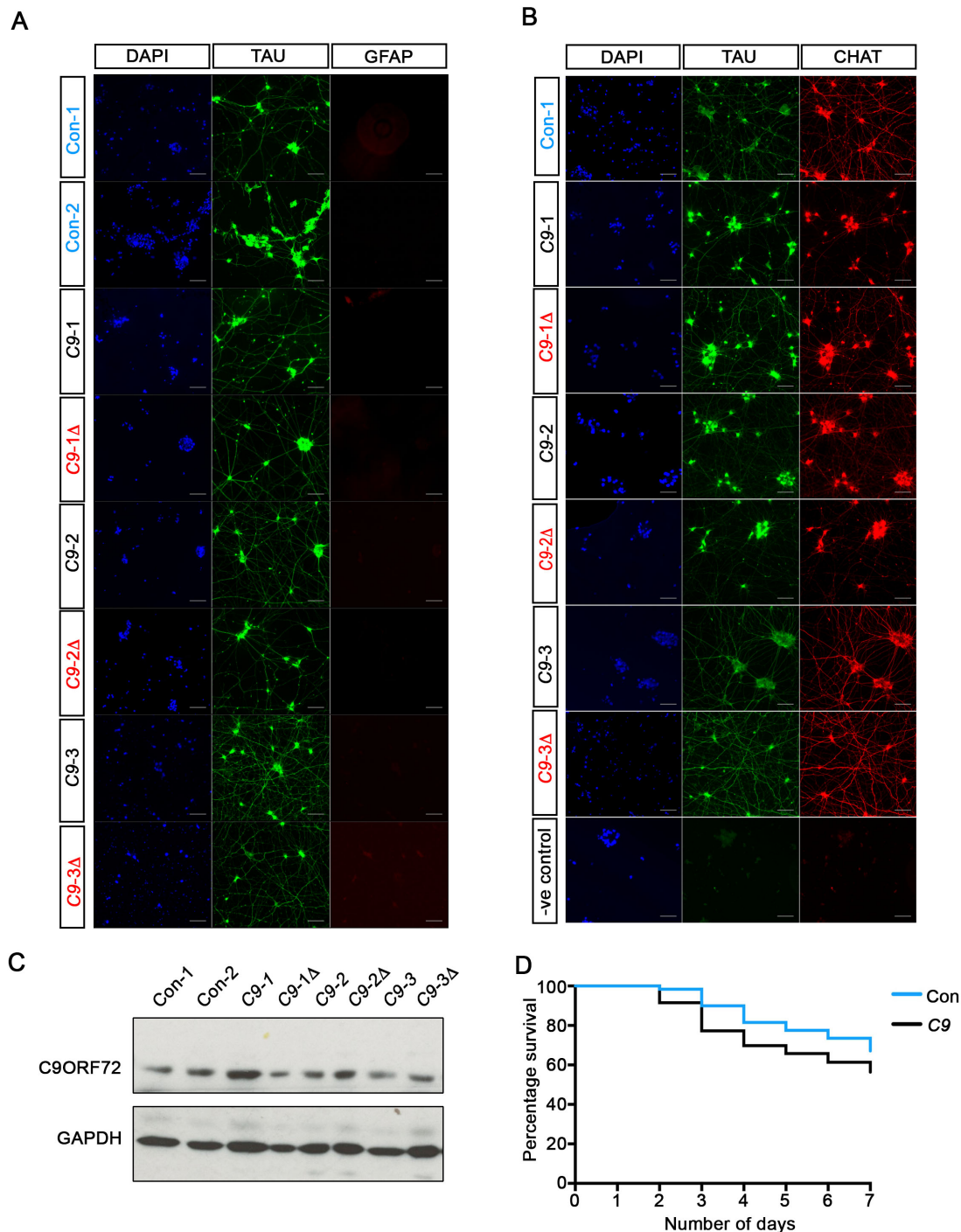
C9-1Δ TTCTTCCTGGATGCCCGCTCCGCCACGCCCAAGTTCTCCGGCA

C9-2Δ TTCTTCCTGGATGCCCGCTCCGCCACGCCCAAGTTCTCCGGCA

C9-3Δ TTCTTCCTGGATGCCCGCTCCGCCACGCCCAAGTTCTCCGGCA

525 **SUPPLEMENTARY FIGURE 1. A**, Repeat primed PCR data depicting the extent of G₄C₂
526 repeat expansions on mutant *C9ORF72* iPSCs. **B**, Karyotype of C9-1Δ, C9-2Δ and C9-3Δ iPSC
527 lines. **C**, C9-1Δ, C9-2Δ and C9-3Δ iPSCs expresses various pluripotency markers (Oct3/4, Tra-
528 1-60). **D**, Sanger sequencing to analyse off-target effects of gRNAs in C9-1Δ, C9-2Δ and C9-
529 3Δ iPSCs.
530

Supplementary Figure 2



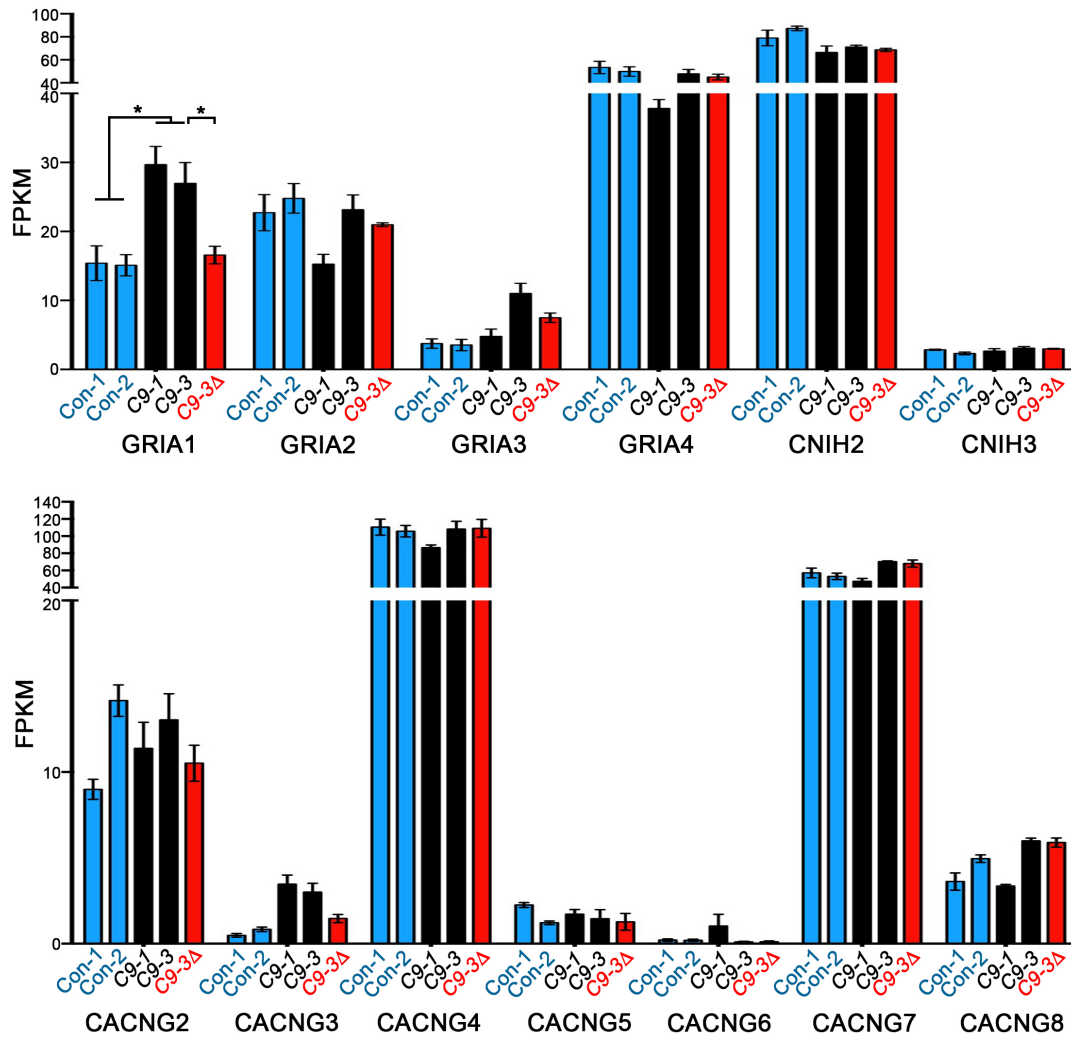
531

532

533 **SUPPLEMENTARY FIGURE 2.** **A**, Representative immunofluorescence images of MNs534 labelled with TAU (neuronal marker) and GFAP (astrocyte marker), scale bar: 50 μm). **B**,535 Representative image of CHAT immunostaining in 3 week old MNs, scale bar: 50 μm. **C**,536 Representative Western blot analysis of *C9ORF72* protein level in control, mutant *C9ORF72*537 and *C9-Δ* iPSC derived MNs. **D**, Longitudinal survival analysis of MNs derived from control538 and mutant *C9ORF72* MNs showed that the G₄C₂ expansion repeats did not affect survival of

539 MNs. Con-1, 53.6±8.5% N=3; Con-2, 63.9±8.9% N=3; C9-1, 53.6±4.9% N=3; C9-3, 46.6±10.4% N=3 at least 35 cells per experiment

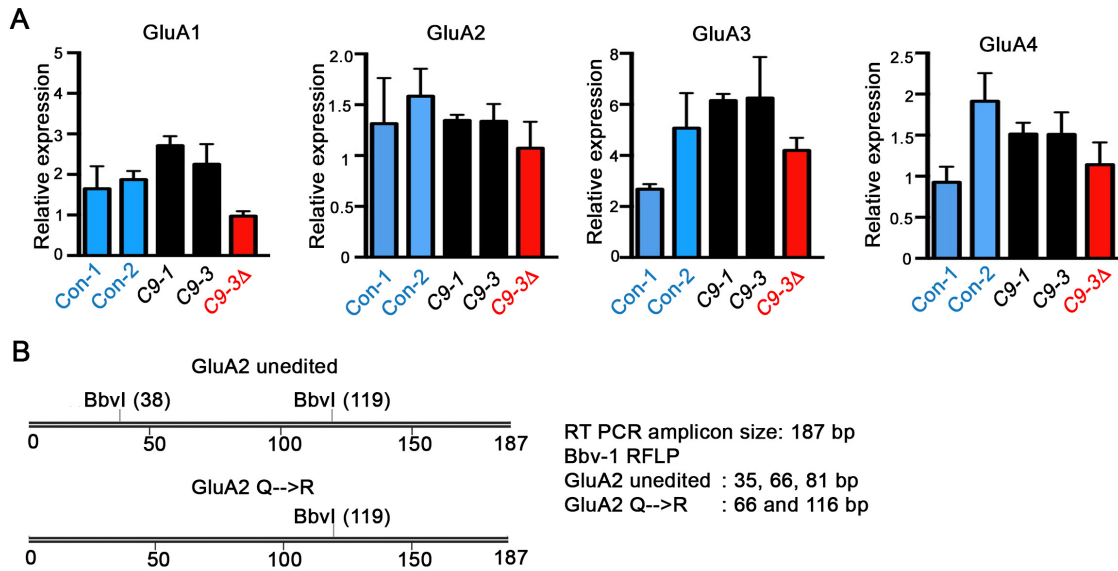
Supplementary Figure 3



540
541
542
543

SUPPLEMENTARY FIGURE 3. RNA-Seq analysis of AMPAR subunits and auxiliary subunits performed on 3-week old control, mutant *C9ORF72*, C9-3Δ MNs (N=3 for all genotypes).

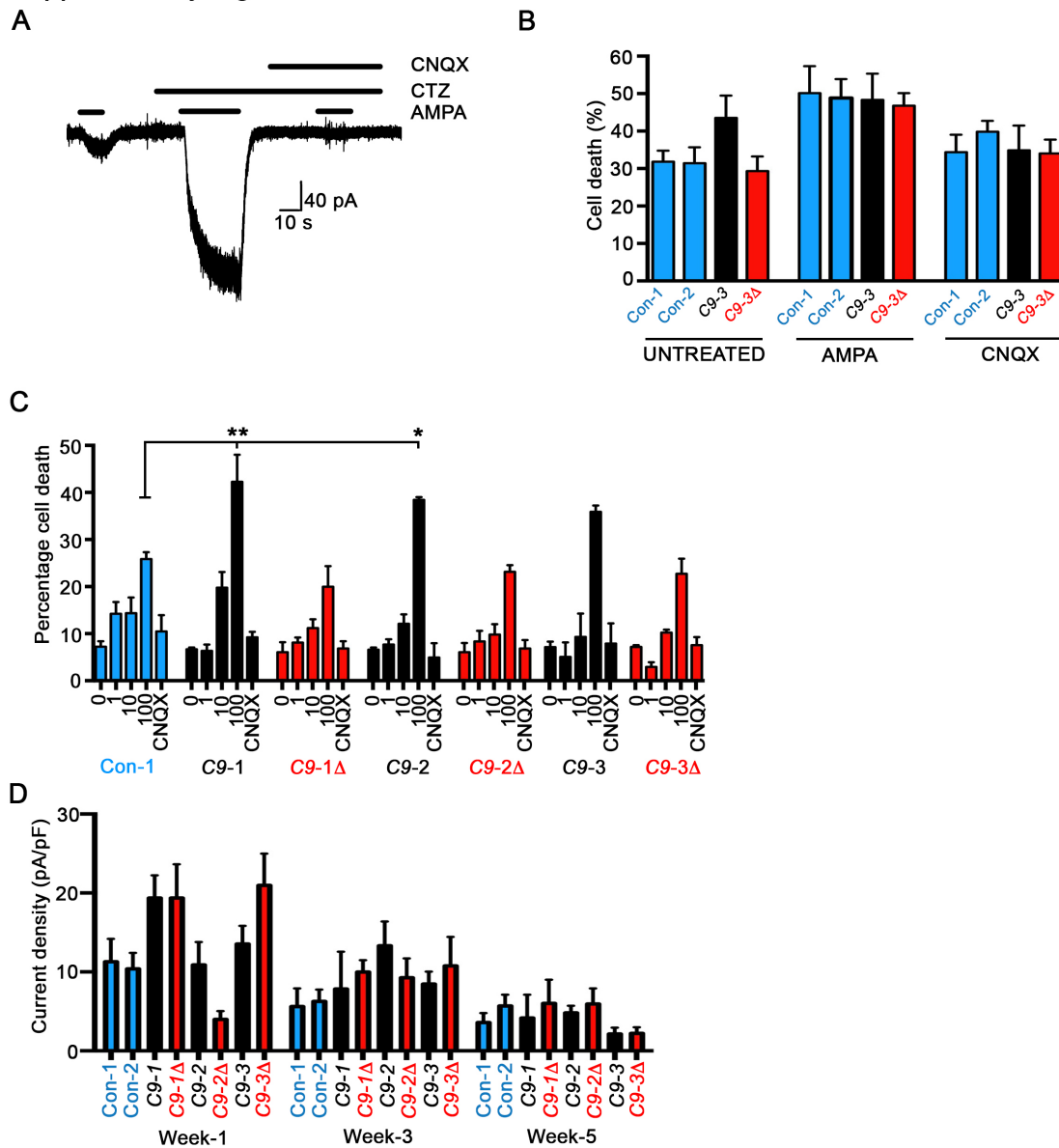
Supplementary Figure 4



544
 545
 546
 547
 548
 549
 550

SUPPLEMENTARY FIGURE 4. **A**, Relative mRNA expression of AMPAR subunits in all cultures examined at Week 1 after differentiation. Data represented as mean \pm s.e.m, Con-1, N=3; Con-2, N=5; C9-1, N=3; C9-3, N=4; C9-3 Δ , N=4. **B**, Restriction fragment length polymorphism (RFLP) strategy to detect the GluA2 A \rightarrow I mRNA post-transcriptional editing using Bbv1 endonuclease.

Supplementary Figure 5

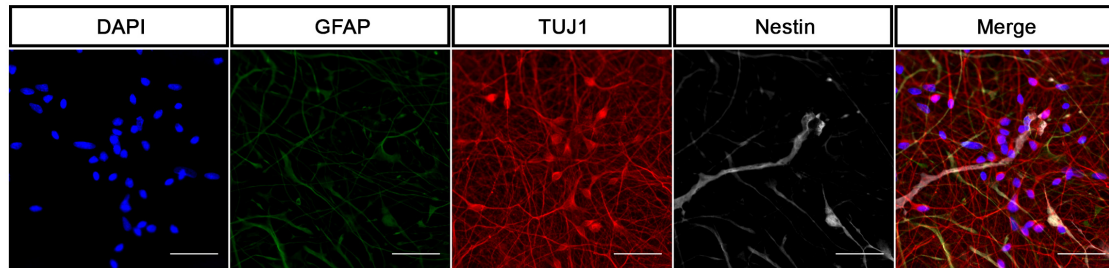


551
 552 **SUPPLEMENTARY FIGURE 5.** A, Whole-cell voltage-clamp recording conducted at -74
 553 mV showing the potentiation of AMPA (10 μM)-mediated currents by cyclothiazide (10 μM),
 554 an AMPAR-selective allosteric potentiator, and subsequent block by CNQX (10 μM). B, Mean
 555 percentage cytotoxicity of 1 week old MNs treated with AMPA and AMPA+CNQX for 24 h.
 556 Data represented as mean \pm s.e.m; Con-1, N=3; Con-2, N=3; C9-3, N=3; C9-3 Δ , N=3. C, Mean
 557 percentage cell death of week 3 MNs treated with different concentrations of AMPA (in the
 558 presence of CTZ) for 24 h. Data represented as mean \pm s.e.m; Con-1, N=3; Con-2, N=3; C9-1,
 559 N=3; C9-1 Δ , N=3; C9-2, N=3; C9-2 Δ , N=3; C9-3, N=3; C9-3 Δ , N=3. Statistical comparisons;
 560 one-way ANOVA with uncorrected Fisher's LSD. D, Mean AMPAR current density
 561 measurements in all lines examined at Week 1, 3 and 5 after differentiation. For all lines at
 562 each time point n=3-16, N=1-4. Statistical difference was not found between patient and
 563 healthy/isogenic MNs (one-way ANOVA with Bonferroni's *post hoc* test)

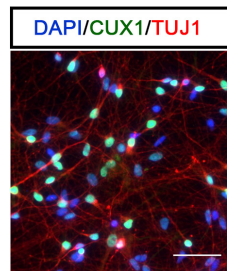
564
 565
 566

Supplementary Figure 6

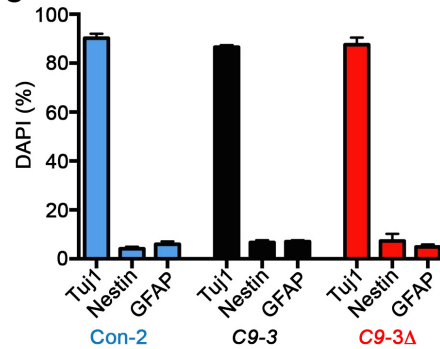
A



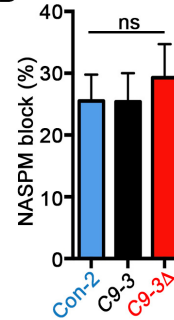
B



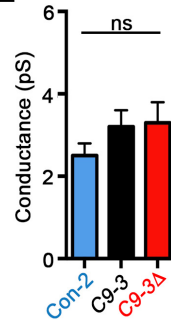
C



D



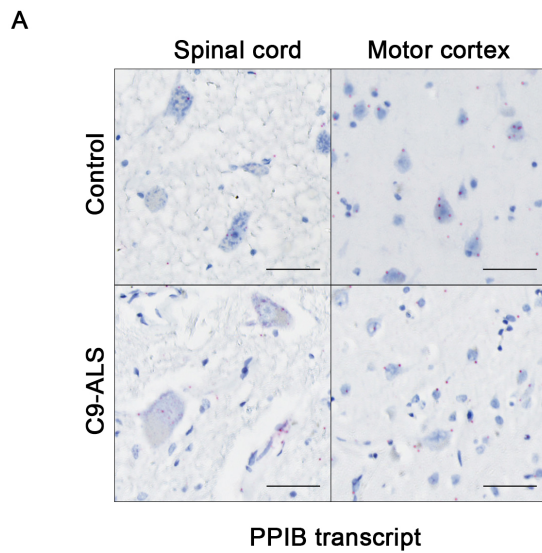
E



567
568
569
570
571
572
573
574
575
576
577

SUPPLEMENTARY FIGURE 6. A-B, Representative images of stainings for 5-week old iPSC derived cortical neurons with TuJ1/GFAP/Nestin (A) and CUX1/TuJ1 (B). C, Basic % TuJ1/Nestin/GFAP with respect to DAPI at 5 weeks. D, Mean percentage NASPM block of AMPA-induced currents in all cortical neurons examined at Week 5 after differentiation. No significant difference was observed between lines (data represented as mean \pm s.e.m; Con-2, n=9, N=3; C9-3, n=7, N=3; C9-3 Δ , n=8, N=3). E, Mean estimated AMPAR γ in all lines examined at Week 5 after differentiation. No significant difference was observed between lines (data represented as mean \pm s.e.m; Con-2, n=14, N=3; C9-3, n=17, N=3; C9-3 Δ , n=17, N=3).

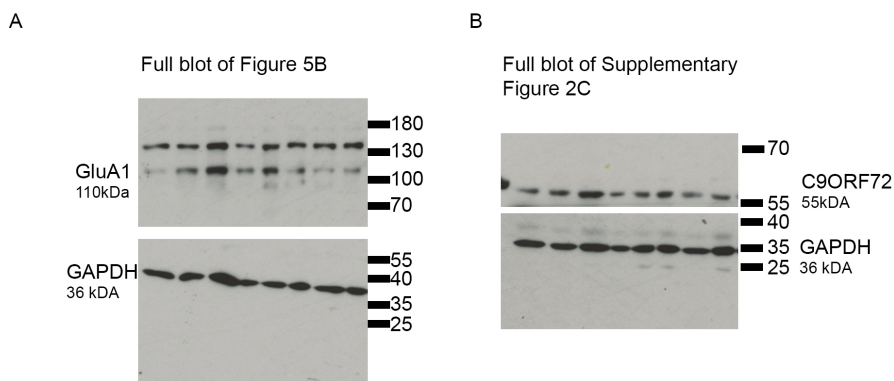
Supplementary Figure 7



578
579
580
581
582
583
584

SUPPLEMENTARY FIGURE 7. Positive control staining of PPIB in human post mortem sections. Representative RNAScope images showing the expression of PPIB in the spinal cord and prefrontal cortex of the same patients presented in Figure 7. Scale bar, 50 μ m.

Supplementary Figure 8



585
586
587

SUPPLEMENTARY FIGURE 8. Full blot of Figure 5B and Supplementary Figure 2C

588

589 **SUPPLEMENTARY TABLE 1: Intrinsic properties of iPSC-derived motor neurons**

iPSC-derived line	Week	Input Resistance (MΩ)	Resting Membrane Potential (mV)	Whole-Cell Capacitance (pF)	Frequency-Input slopes
Con-1	1	1982 ± 172	-56.6 ± 2.1	16.7 ± 1.6	0.121 ± 0.07
	3	1206 ± 169 ^a	-55.8 ± 2.4	18.5 ± 2.0	
	5	701 ± 66 ^{a,b}	-60.5 ± 1.6	23.0 ± 1.9	
Con-2	1	1456 ± 156	-49.2 ± 2.5	15.3 ± 0.8	0.175 ± 0.03
	3	841 ± 88 ^a	-51.6 ± 2.0	20.3 ± 1.7	
	5	693 ± 50 ^a	-59.1 ± 21.6	28.1 ± 2.1 ^a	
C9-1	1	1596 ± 189	-53.7 ± 1.9	14.8 ± 1.3	0.156 ± 0.03
	3	1393 ± 139	-59.6 ± 1.9	23.7 ± 2.4	
	5	1003 ± 85 ^a	-59.9 ± 1.4	25.9 ± 2.0 ^a	
C9-1Δ	1	1159 ± 96	-39.3 ± 1.2	11.8 ± 1.1	0.163 ± 0.06
	3	983 ± 144	-53.8 ± 1.9 ^a	24.4 ± 4.5 ^a	
	5	793 ± 59 ^a	-52.8 ± 1.4 ^a	18.1 ± 1.4	
C9-2	1	1824 ± 195	-37.8 ± 2.1	19.4 ± 2.4	0.136 ± 0.04
	3	801 ± 107	-46.2 ± 3.8	34.7 ± 3.4 ^a	
	5	682 ± 43 ^b	-51.7 ± 2.4 ^{a,b}	40.7 ± 2.0 ^a	
C9-2Δ	1	1406 ± 183	-38.3 ± 2.1	24.2 ± 2.3	0.082 ± 0.06
	3	685 ± 97 ^a	-47.9 ± 2.6	29.4 ± 2.9	
	5	646 ± 52 ^a	-52.8 ± 1.4 ^{a,b}	24.1 ± 2.7	
C9-3	1	1854 ± 218	-54.9 ± 2.0	17.0 ± 1.2	0.130 ± 0.04
	3	1335 ± 140 ^a	-52.2 ± 2.3	16.3 ± 1.5	
	5	816 ± 54 ^{a,b}	-59.1 ± 1.2 ^b	23.1 ± 1.2 ^{a,b}	
C9-3Δ	1	2118 ± 189	-54.7 ± 2.1	12.4 ± 1.0	0.221 ± 0.03
	3	959 ± 108 ^a	-61.4 ± 2.7	27.6 ± 3.4 ^a	
	5	757 ± 52 ^a	-65.2 ± 1.1 ^a	26.9 ± 1.2 ^a	

590

591 **SUPPLEMENTARY TABLE 1. Intrinsic properties recorded from iPSC-derived motor**
592 **neurons.** Mean input resistance, resting membrane potential and whole-cell capacitance data
593 for each line obtained at weeks 1, 3 and 5. Data points were obtained from a range of 6-99 cells
594 derived from 2-9 *de novo* batches of cells. Statistical data (one-way ANOVA with Bonferroni's
595 *post hoc* test) presented with respect week 1 (^a signifies p>0.05) and week 3 data (^b signifies
596 p>0.05). Mean frequency-input slope data for repetitively firing Week 5 cells from each iPSC-
597 derived line. Data obtained from 3-39 cells. Statistical significance is not observed between
598 patient versus healthy/isogenic lines (one-way ANOVA with Bonferroni's *post hoc* test).

599

600 **SUPPLEMENTARY DATA 1: List of genes that are significantly upregulated in**
601 ***C9ORF72* mutant motor neurons (attached excel sheet)**

602

603 **SUPPLEMENTARY DATA 2: List of genes that are significantly downregulated in**
604 ***C9ORF72* mutant motor neurons (attached excel sheet)**

